

Evaluation of parametrizations of microphysical and optical properties for radiative flux computations in climate models using TOVS-ScaRaB satellite observations

C. J. Stubenrauch, F. Eddouia¹, and J. M. Edwards²

¹*C.N.R.S. / IPSL - Laboratoire de Météorologie Dynamique, Ecole Polytechnique, Palaiseau, France*

²*Met Office, Fitzroy Road Exeter EX1 3PB, United Kingdom*

Abstract

In this study we have determined the most appropriate parametrizations of microphysical and optical properties of cirrus clouds for radiative flux computations in climate models. Atmospheric and cirrus properties retrieved from TOVS observations are given as input to the radiative transfer model to simulate fluxes at the top of the atmosphere. These simulated fluxes are then compared to time space co-located fluxes retrieved from ScaRaB observations. Three parametrizations of cirrus ice crystal optical properties, developed by Mitchell, Baran and Fu, are used for the simulations. These parametrizations are based on different physical approximations and different hypotheses on crystal shape. The first two parametrizations suppose ice crystals to have the shape of aggregates and the last suppose crystals to have the shape of hexagonal columns. Our quantitative study shows that the parametrization assuming hexagonal columns seems to be plausible only for cirrus with small ice water path (IWP). The assumption of aggregates fits the simulated cirrus albedos for larger IWP. From our analysis we conclude that cirrus parametrizations in climate models should use an increase of effective ice crystal diameter (D_e) with IWP instead of an increase of D_e with temperature.

Introduction

Cirrus clouds occur widely in the atmosphere and play an important role in the climate system. Due to their complex microphysical characteristics (consisting of non-spherical ice crystals of various shapes and sizes), however, their physical and radiative properties are still not completely understood. Therefore most climate models still use ice spheres or hexagonal columns in the computation of cirrus radiative properties.

Nevertheless, the effect of replacing spheres by more realistic ice crystal shapes in the radiation computations of a GCM can lead to large changes in the radiative longwave (LW) and shortwave (SW) fluxes (up to 10 and 25 Wm^{-2} respectively) which themselves drive the dynamics of the atmosphere (Kristjansson et al. 2000). For reliable predictions of climate change it is therefore essential to find realistic assumptions on ice crystal shapes and sizes which form the cirrus clouds and to compute their radiative properties accurately.

TOVS – ScaRaB data set

The TOVS Path-B data set (Scott et al. 1999) provides atmospheric temperature and water vapor profiles as well as cloud and surface properties at a spatial resolution of 1° latitude x 1° longitude, from 1987 to 1995. Their relatively high spectral resolution yields reliable cirrus properties, day and

night (Stubenrauch et al. 1999). For large-scale semi-transparent cirrus (visible optical thickness between 0.7 and 3.8) observed from NOAA-10 satellites bulk microphysical properties have been retrieved, using spectral cirrus emissivity differences between 11 and 8 μm (Rädel et al. 2003, Stubenrauch et al. 2004a).

The ScaRaB radiometer on board the Russian Meteor-3/7 satellite provided Earth Radiation Budget observations from March 1994 to February 1995 (Kandel et al. 1998). The inclination of the orbit (82.6°) is such that all local hours are observed within 104 days. In addition to the two ERBE-like broad-band LW and SW channels, the ScaRaB instrument has two narrow-band infrared (IR) and visible (VIS) channels for improved cloud scene identification.

For cloud detection and for the determination of their properties the ISCCP method (Rossow and Garder 1993, Rossow and Schiffer 1999) was applied to the ScaRaB IR and VIS radiances. For complementary cloud property information, the ScaRaB data set was collocated with original ISCCP data during daytime. The ScaRaB-ISCCP daytime data set has then been collocated with quasi-simultaneous ($\Delta t < 30$ minutes) TOVS large-scale semi-transparent cirrus data from NOAA-11 and NOAA-12 observations. For the period from March 1994 until August 1994 we are left with 4130 cases: 1570 cases over land and 2560 cases over ocean. The sun zenith angle lies between 50° and 70° and relative azimuth is less 40° (forward scattering) or larger than 140° (backward scattering). For the cirrus radiative flux analysis we use the SW albedo of 1570 isolated cirrus over ocean, which have been selected as cirrus with the IR emissivity computed from the ScaRaB VIS optical thickness close to the TOVS IR emissivity (Stubenrauch et al. 2004a, Eddounia 2004). The SW albedo has been computed from the SW reflectance measured under a specific viewing angle by applying Angular Direction Models (ADMs) based on cloud properties and developed using a neural network approach and Monte Carlo radiative transfer simulations (Briand 2000).

Cirrus radiative flux analysis

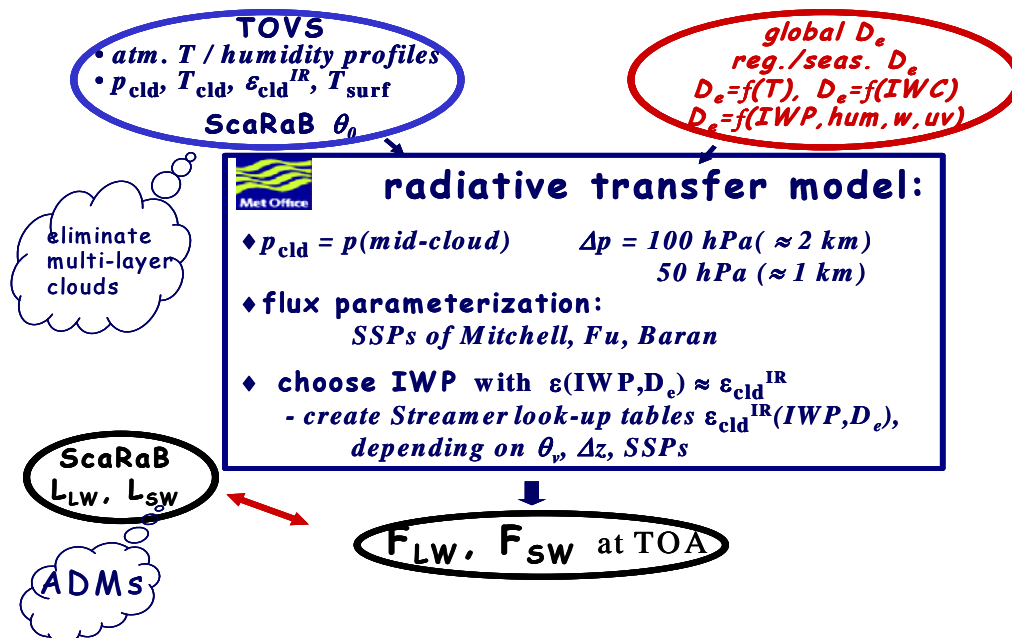


Fig. 1: Scheme of cirrus radiative flux analysis.

Fig. 1 presents the analysis scheme. For this analysis we use quasi-simultaneous data of atmospheric and cirrus properties from TOVS and their associated radiative fluxes at the top of the atmosphere

(TOA) from ScaRaB as well as the MetOffice radiative transfer model (Edwards and Slingo 1996). Cirrus IR effective emissivity, cloud-top pressure and temperature are given as input to the model, together with an expression for the effective ice crystal diameter D_e . Atmospheric temperature and humidity profiles for the radiative transfer computation are taken from the Thermodynamic Initial Guess Retrieval (TIGR) data set (Chevallier et al. 1998) for the situation closest to the TOVS observation. One can choose between three different flux parametrizations using single scattering properties of ice crystals with an assumed shape of hexagonal columns (Fu 1996), aggregates made of plates (Mitchell et al. 1996) and aggregates made of columns (Baran et al. 2003). The cloud geometrical thickness is fixed to 100 hPa ($\approx 2\text{km}$). The ice water path (IWP) is computed from the cirrus IR effective emissivity by using look-up tables established by radiative transfer computations (Key and Schweiger 1998), depending on IR effective emissivity and D_e . The single scattering properties used in these radiative transfer computations have to be the same as in the chosen flux parameterisation. The simulated radiative fluxes are then compared to those observed by ScaRaB.

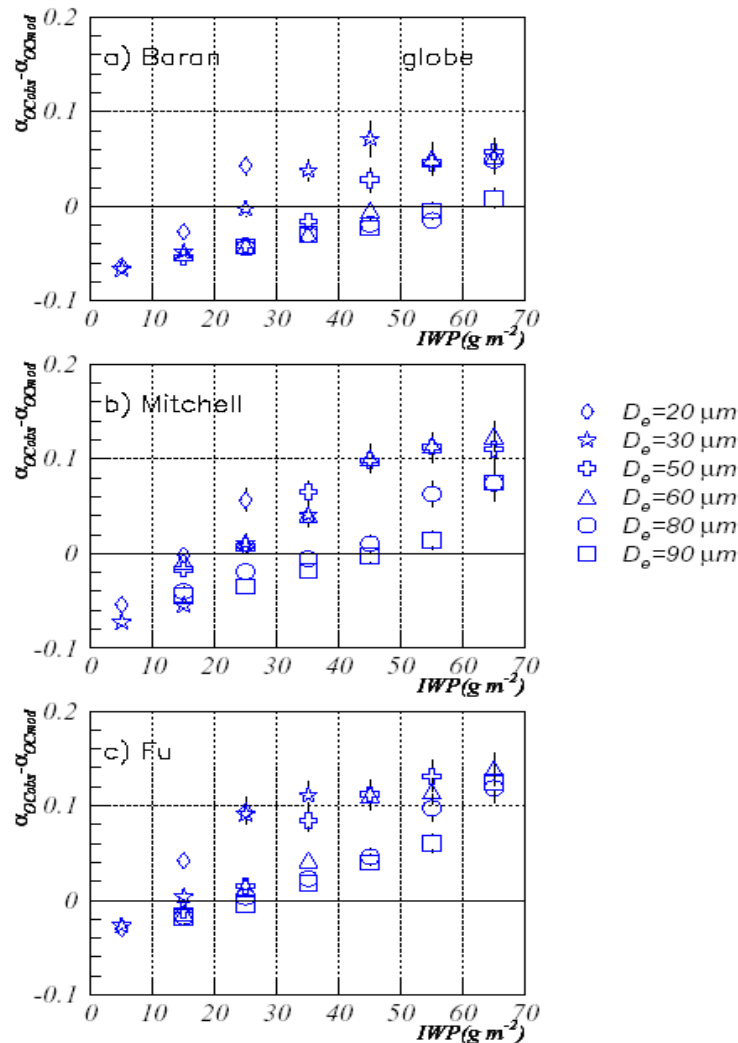


Fig. 2: Difference of observed and simulated isolated cirrus SW albedo as function of IWP. Simulations have been made by using single scattering property parametrizations a) for ice aggregates made of columns (Baran), b) ice aggregates made of plates (Mitchell) and c) for ice crystals with the shape of hexagonal columns (Fu), with D_e between 20 and 90 μm .

Best suited parametrizations of D_e for climate model simulations

We first evaluate the coherence of the single scattering property parametrizations in the thermal and solar spectrum. Therefore we compare the simulated cirrus SW albedo to the observed cirrus SW albedo as a function of IWP, varying D_e between 20 and 90 μm . Figs. 2 present the difference between observed and simulated cirrus SW albedo as function of IWP for six different D_e 's, assuming the ice crystals to have the shape of aggregates or hexagonal columns. From these figures we deduce the following:

- The parametrization assuming ice crystals as hexagonal columns (by Fu) seems to be plausible only for small IWP.
- If one assumes ice crystal aggregates (parametrization by Baran), the simulations fit the observed cirrus SW albedo within less than 2% by increasing D_e from 20 to 90 μm for IWP between 25 and 65 g m^{-2} .

For a more quantitative analysis we have computed for each cirrus observation an average $\langle D_e \rangle_{IWP}$, by varying D_e between 10 and 90 μm and weighting by the squared inverse of the difference between observed and simulated SW albedo, as:

$$\langle D_e \rangle_{IWP} = \frac{\sum_{i=1}^9 \frac{D_e^i}{[\alpha_{SWobs} - \alpha_{SWsim}(D_e^i)]^2}}{\sum_{i=1}^9 \frac{1}{[\alpha_{SWobs} - \alpha_{SWsim}(D_e^i)]^2}}$$

with $D_e^i = \{10\mu\text{m}, 20\mu\text{m}, \dots, 90\mu\text{m}\}$

Fig. 3 presents $\langle D_e \rangle_{IWP}$ as a function of IWP for the three parametrizations. For all shape assumptions D_e which fits best the observations if it increases with IWP.

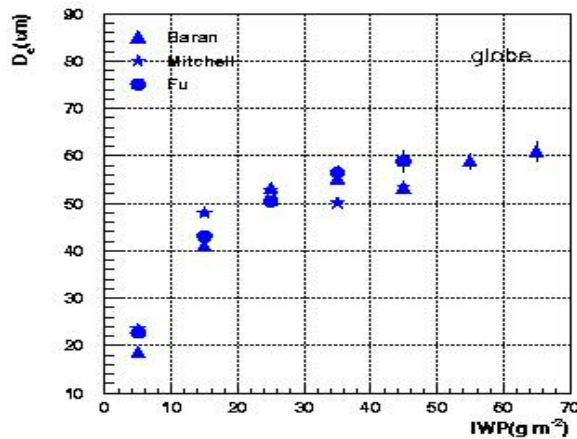


Fig. 3: $\langle D_e \rangle_{IWP}$ as a function of IWP for the three ice crystal single scattering property parametrizations.

In a last step we test the best suited parametrization of D_e for cirrus radiative flux computations by comparing distributions of differences between observed cirrus SW albedo and simulated cirrus SW albedo, assuming

- 1) a constant $D_e = 55 \mu\text{m}$, the global average from TOVS observations (Rädel et al. 2003)
- 2) D_e increasing with IWP as shown in Fig. 3
- 3) D_e increasing with cloud temperature as it is actually used in the MetOffice climate model.

From Figs. 4 we conclude that the best suited D_e parametrization for cirrus radiative fluxes would be D_e increasing with IWP. A more detailed description of the analysis and results is given in (Eddounia 2004) and a publication in English is in preparation.

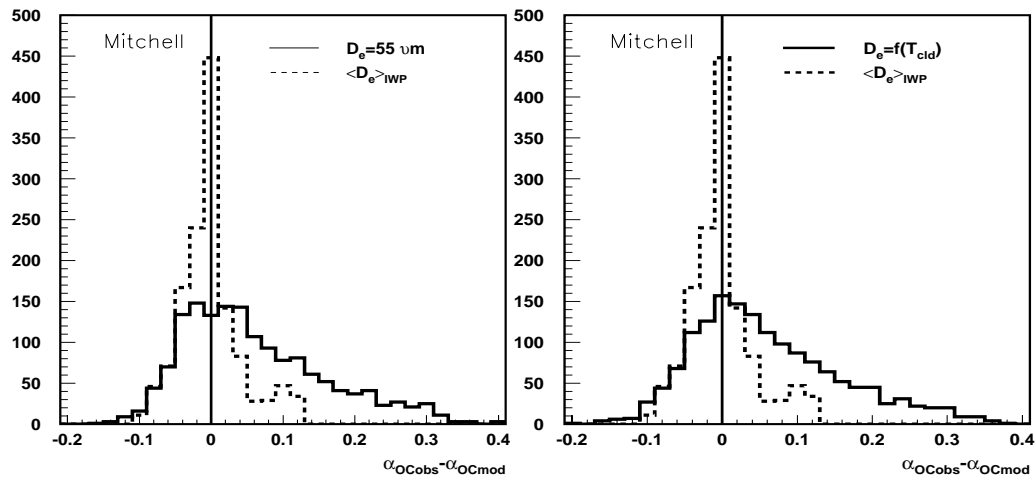


Fig. 4: Distributions of differences between observed cirrus SW albedo and simulated cirrus SW albedo, assuming constant D_e and D_e increasing with IWP (left) and assuming D_e increasing with IWP and D_e increasing with cloud temperature (right).

References

- Baran, A.J., Havemann, S., Francis, P.N. and Watts, P.D. 2003. A consistent set of single scattering properties for cirrus cloud: a test using radiance measurements from a dual-viewing multi-wavelength satellite-based instrument. *J. Quant. Spectrosc. Rad. Trans.*, **79-80**, 707-720.
- Briand, V. 2000. Vers une meilleure exploitation des observations satellitales pour l'étude de l'effet radiatif des nuages. Ph. D. thesis, University of Paris VI, pp. 129 (available from LMD, Palaiseau).
- Chevallier, F., Cheruy, F., Scott, N.A., and Chédin, A. 1998. A neural network approach for a fast and accurate computation of longwave radiative budget. *J. Appl. Meteor.*, **37**, 1385-1397.
- Eddounia, E. 2004. La microphysique des cirrus à l'échelle du globe: Corrélation avec les propriétés atmosphériques pour une meilleure représentation dans les modèles de climat. Ph. D. thesis, Ecole Polytechnique, pp. 155 (available from LMD, Palaiseau).
- Edwards, J.M. and Slingo, A. 1996. Studies with a flexible new radiation code: I. Choosing a configuration for a large-scale model. *Q. J. Roy. Meteorol. Soc.*, **122**, 689-719.
- Fu, Q., 1996. An accurate parameterization of the solar radiative properties of cirrus clouds for climate models. *J. Climate*, **9**, 2058-2082.
- Kandel, R. and Coauthors 1998. The ScaRaB earth radiation budget dataset. *Bull. Amer. Meteor. Soc.*, **79**, 765-783.
- Key, J. and Schweiger, A. 1998. Tools for atmospheric radiative transfer: Streamer and FluxNet. *Computer & Geosciences*, **24**, 443-451.
- Kristjansson, J.-E., Edwards, J.M. and Mitchell, D.L. 2000. The impact of a new scheme for the optical properties of ice crystals on the climates of two GCMs. *J. Geophys. Res.*, **105**, 10063-10079.
- Mitchell, D.L., Macke, A. and Liu, Y. 1996. Modelling Cirrus Clouds: II) Treatment of radiative properties. *J. Atmos. Sci.*, **53**, 2967-2988.

- Rädel, G., Stubenrauch, C.J., Holz, R. and Mitchell, D.L. 2003. Retrieval of Effective Ice Crystal Size in the Infrared : Sensitivity Study and Global Measurements from the TIROS-N Operational Vertical Sounder. *J. Geophys. Res.* **108**, 10.1029/2002JD002801.
- Rossow, W.B. and Garder, L.C. 1993. Cloud detection using satellite measurements of infrared and visible radiances for ISCCP. *J. Climate*, **6**, 2341-2369.
- Rossow, W.B. and Schiffer, R.A. 1999. Advances in understanding clouds from ISCCP. *Bull. Amer. Meteor. Soc.*, **80**, 2261-2287.
- Scott, N.A., Chédin, A., Armante, R., Francis, J., Stubenrauch, C.J., Chaboureau, J.-P., Chevallier, F., Claud, C. and Chéruy, F. 1999. Characteristics of the TOVS Pathfinder Path-B data set. *Bull. Amer. Meteor. Soc.*, **80**, 2679-2701.
- Stubenrauch, C.J., Rossow, W.B., Scott, N.A. and Chédin, A. 1999a. Clouds as seen by Infrared Sounders (3I) and Imagers (ISCCP): Part III) Spatial Heterogeneity and Radiative Effects. *J. Climate*, **12**, 3419-3442.
- Stubenrauch, C.J., Chédin, A., Armante, R. and Scott, N.A. 1999b. Clouds as seen by Infrared Sounders (3I) and Imagers (ISCCP): Part II) A New Approach for Cloud Parameter Determination in the 3I Algorithms. *J. Climate*, **12**, 2214-2223.
- Stubenrauch, C.J., Eddounia, F. and Rädel, G. 2004a. Correlations between microphysical properties of large-scale semi-transparent cirrus and the state of the atmosphere. *Atmos. Res.*, **72**, 403-423.
- Stubenrauch, C.J., and the CIRAMOSIA team 2004b. final report on the European Environmental project EVK2-CT-2000-00063, 99 pp., available at: <http://www.lmd.polytechnique.fr/CIRAMOSIA/Welcome.html>.